REVIEW

Welding residual stresses in ferritic power plant steels

J. A. Francis*[1], H. K. D. H. Bhadeshia[2] and P. J. Withers[1]

Many of the degradation mechanisms relevant to power plant components can be exacerbated by stresses that reside within the material. Good design or structural integrity assessments require therefore, an accounting of residual stresses, which often are introduced during welding. To do this it is necessary to characterise the stresses, but this may not be possible in thick components using non-destructive methods. These difficulties, and a paucity of relevant engineering data, have led to an increasing emphasis on the development and validation of suitable modelling tools. Advances are prominent in the estimation of welding residual stresses in austenitic stainless steels. The progress has been less convincing in the case of ferritic alloys, largely due to the complexities associated with the solid state phase transformations that occur in multipass welding. We review here the metallurgical issues that arise in ferritic steel welds, relate these to the difficulties in calculating residual stresses, and highlight some stimulating areas for future research.

Keywords: Phase transformation, Power plant, Residual stress, Steel, Structural integrity, Weld

Introduction

Residual stresses are those which are not required for a engineering structure to maintain equilibrium with its environment.[1] Although they can have many different origins, residual stresses are always the result of some form of misfit; either between different parts, different regions within the same part, or even different phases within a microstructure.[2] Welding residual stresses arise as a consequence of the heterogeneous application of energy and localised fusion. When the fused region solidifies, the accompanying contraction exerts a pull on the surrounding material which may be prevented from complying by constraint. The contraction of the weld metal may be too large to sustain elastically, so plastic deformation is induced. All this means that in the absence of transformation effects, significant tensile stresses reside in the near weld region after the component has reached thermal equilibrium.[3]

Many of the degradation mechanisms relevant to power plant components can be accelerated by the presence of residual stresses. Tensile welding residual stresses in particular can contribute to fatigue crack development in a structure even under compressive cyclic loading.[4,5] Similarly, stress corrosion cracking can occur in austenitic weldments if the sum of the applied and residual stress exceeds a threshold.[6] Residual stresses are also known to affect fracture processes,[7,8] and have been shown to accelerate the onset of creep damage.[9,10] It is not surprising therefore, that significant resources are devoted to the inclusion of residual stresses in engineering integrity assessments.[11–13]

Many plant components are subjected to externally applied loads at elevated temperatures over design lives that span decades. Reactor pressure vessels, headers and the main steam pipe in fossil fired boilers are all thick walled components designed to withstand harsh operating environments. Unfortunately, it is extremely difficult to measure bulk residual stresses non-destructively in such thick components, and this has contributed to a paucity of engineering data.[14] Instead, the focus is often placed on the validation of numerical modelling techniques so that stresses can be estimated. While a number of challenges remain, there have been examples of the successful implementation of numerical models for welding residual stress development in austenitic stainless steels.[15,16] By comparison, modelling activities focussing on ferritic steels are less advanced, largely due to the complexities that are introduced by the solid state phase transformations that take place during multipass welding.

The purpose of this article is to review recent progress in understanding the development of welding residual stresses in ferritic steels. We begin with a description of the metallurgy, before addressing the consequences of solid state phase transformations on stresses induced by welding. Attention is then given to published stress measurements. Finally, an assessment is made of the status of weld modelling and here we highlight some exciting challenges for future work. It is hoped that this review will provide a useful summary of the issues relating to ferritic welds, and serve as a stimulus for

[1]School of Materials, University of Manchester, Grosvenor Street, Manchester M1 7HS, UK
[2]Department of Materials Science and Metallurgy, University of Cambridge, Pembroke Street, Cambridge, CB2 3QZ, UK

*Corresponding author, email John.Francis@manchester.ac.uk

Published by Maney on behalf of the Institute
Received 20 April 2007; accepted 22 May 2007
DOI 10.1179/174328407X213116

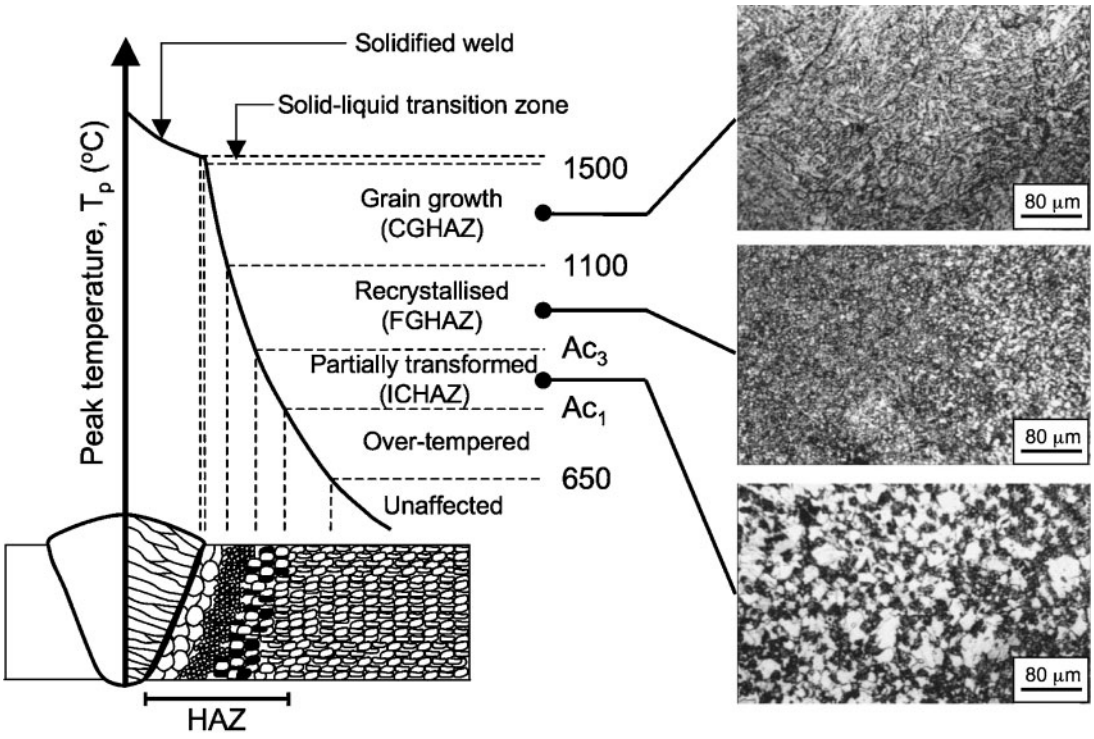

1 Metallurgical zones in single pass weld, categorised according to maximum local temperature:[19] micrographs, after Ref. 20, correspond to weld in 2·25Cr–1Mo steel

advances that ultimately translate into engineering practice.

Weld metallurgy

Fusion welding involves the localised injection of intense heat and its dissipation by conduction into the parent material. The weld microstructure at each location is therefore closely related to the thermal history.[17] The different zones and their characteristics have been described for a single pass weld by Mannan and Laha,[18] and are shown in Fig. 1.[19,20] Regardless of the primary solidification structure, the fusion zone in low alloy steels transforms to austenite at a temperature not far from the solidification point,[21] and then undergoes a solid state transformation to a structure that will depend on both the hardenability of the alloy and the cooling rate. Adjacent to the fusion zone is a heat affected zone (HAZ); a region that is not heated sufficiently to cause melting, but nevertheless is altered by the welding thermal cycle. As indicated in Fig. 1, the HAZ can be subdivided according to the extent to which grain growth and austenitisation occur; into a coarse grained zone (CGHAZ), a fine grained zone (FGHAZ), an intercritical zone (ICHAZ) and over tempered base metal.

Fusion welding of thick walled components necessarily involves many weld passes to fill up the joint. Weld beads covered by other passes then experience multiple heat pulses and a further subdivision of metallurgical zones. Some of the possible combinations of thermal cycles are illustrated in Fig. 2.[22,23] With regard to the sequence shaded dark grey in Fig. 2, the initial intercritical heating cycle may not have a significant effect on the final microstructure, since the subsequent cycle introduces a much higher peak temperature at that location. However, other sequences can have significant and detrimental effects. For example, the intercritically reheated CGHAZ is the zone of the CGHAZ which is only partly reaustenitised during a subsequent thermal cycle and is shaded black in Fig. 2. In some steels a concentration of austenite stabilisers, such as carbon,

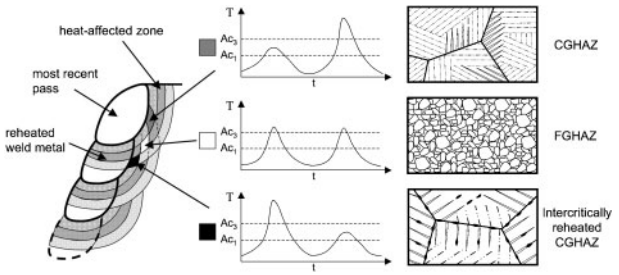

2 Examples of thermal cycles in multipass weld, adapted from Refs. 22 and 23

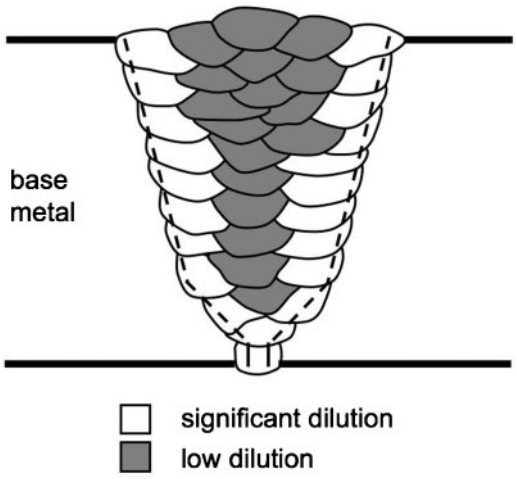

3 Variation in dilution of filler metal in power plant weld

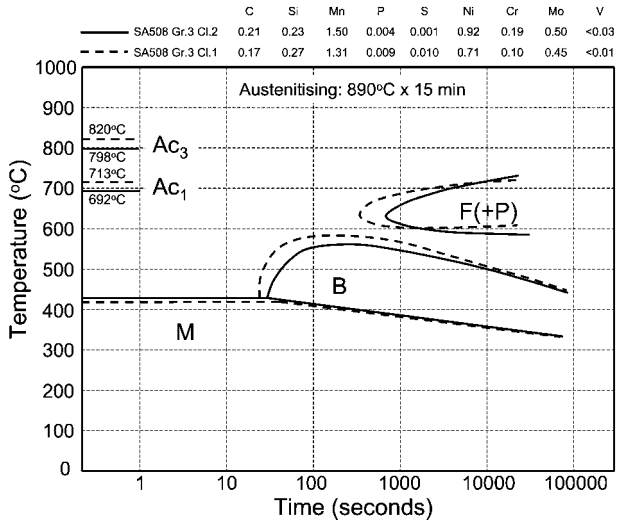

4 Curves of CCT for class 1 (solid lines) and class 2 (broken lines) of grade 3 SA508 reactor pressure vessel steel[30]

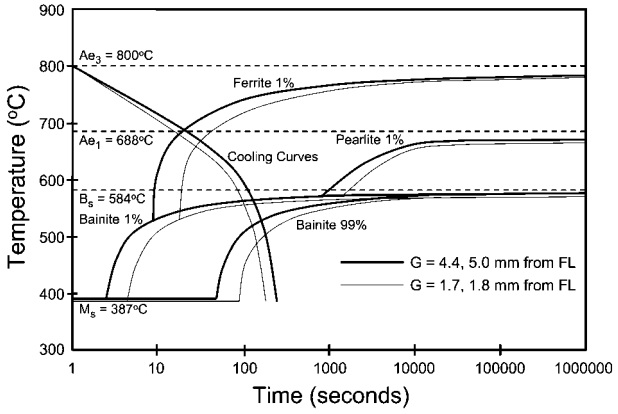

5 Calculated CCT curves for different locations in HAZ of SA508 grade 3, class 1 reactor pressure vessel steel as consequence of differing prior austenite grain size: cooling curves corresponding to these locations are also shown[37]

can occur in the regions that are reaustenitised and, upon cooling, these locations transform into hard microstructures associated with poor toughness, the so called local brittle zones. Given that the austenite in the CGHAZ would have originally been coarse, the decline in toughness in the intercritically reheated CGHAZ can be marked.[24,25]

Filler metals for ferritic steels are generally selected to achieve an appropriate balance between strength and toughness, or to mitigate against toughness related problems such as cold cracking.[26] Other factors may also be relevant, such as with 9–12Cr creep resistant steels, where it is important to avoid the formation of δ-ferrite at high temperatures yet still achieve a complete transformation to martensite at ambient temperature.[27] The design requirements for weld filler metals generally necessitate a chemical composition that differs from the parent material. Thus, in a multipass weld, the composition of one weld bead can vary from the next as a consequence of changes in dilution levels. A schematic representation of how dilution might vary in a typical power plant steel weld is given in Fig. 3. The extent to which dilution might influence microstructure will depend on the mismatch between the compositions of the filler metal and parent material. However, in microalloyed steels, even a relatively small change in composition due to dilution has been shown to significantly affect weld toughness.[28]

Austenite that forms in the fusion zone after solidification, and in the HAZ as a consequence of material being heated above the Ac_1 temperature, will generally transform upon cooling to some combination of ferrite, pearlite, Widmanstätten ferrite, bainite or martensite. If the residual stresses in ferritic welds are to be predicted then it is necessary to understand which transformations are likely to occur, and the temperatures at which they will occur[29] because each of these phase changes is associated with a transformation strain. In the context of welding thermal cycles, the most convenient presentation of the kinetics of these transformations is a continuous cooling transformation (CCT) diagram. The CCT diagrams and chemical compositions for two different classes of a (grade 3 SA508) reactor pressure vessel steel are shown in Fig. 4.[30] Even though there are only minor differences in chemical composition between the two steels, there are noticeable differences between the transformation curves, as well as the respective Ac_1 and Ac_3 temperatures. Indeed the two most significant influences on CCT diagrams are the steel composition and the prior austenite grain size.[31] The sensitivity to composition, as is illustrated in Fig. 4, suggests that models for residual stresses in multipass welds would need to account for the effects of dilution. The effects of austenite grain size are significant in the context of welds because of the spatial variation of peak temperature within the HAZ leading to corresponding variations in grain or precipitate size.

The experimental determination of CCT diagrams using techniques such as dilatometry or differential scanning calorimetry can be tedious. One way of estimating these is a semi-empirical model for hardenable steels developed by Kirkaldy and Venugopalan,[32] and later refined by Li *et al.*[33] The form of the model is based on formulae for isothermal transformations described by Zener[34] and Hillert,[35] which can be expressed as

$$\tau(X,T)=\frac{F(C,Mn,Si,Ni,Cr,Mo,G)}{\Delta T^{n}\exp\left(-\frac{Q}{RT}\right)}S(X) \qquad (1)$$

where τ is the time delay required for the transformation to proceed to a fraction of completion X, at constant temperature T; F is a function of steel composition and ASTM number for grain size G; ΔT is the undercooling; Q is the activation energy for the steel, R is the gas constant, T the absolute temperature and $S(X)$ is a reaction rate term that approximates the sigmoidal effect of phase transformations.[33] Li and co-workers examined the TTT diagrams for many steels and developed empirical expressions for the function F, for ferritic, pearlitic and bainitic transformations. As with the Kirkaldy model, the degree of undercooling is calculated with respect to the Ae_3 and Ae_1 temperatures for the ferritic and pearlitic transformations respectively, and with respect to the bainite start temperature B_S, for bainitic transformations. Li and co-workers estimated the martensite start temperature M_S, with an empirical expression due to Andrews.[36] Once expressions were

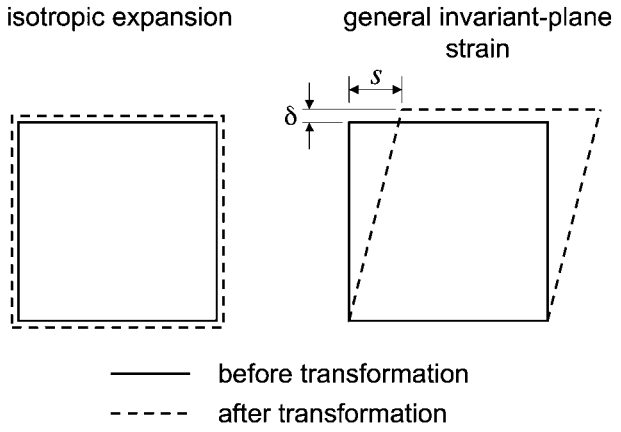

6 Nature of reconstructive transformations (left) and displacive transformations (right) from austenite on cooling: for bainite and martensite $s \approx 0{\cdot}22$–$0{\cdot}26$ and $\delta \approx 0{\cdot}02$–$0{\cdot}03$ (Ref. 39)

obtained for each transformation, Li *et al.* suggested that critical cooling rates for the formation of martensite, for example, could be determined by the larger of the rates for the formation of 1% ferrite or 1% bainite, with equations of the form

$$CCR_{1\%F} = \int_{Ae_3}^{B_s} \frac{dT}{\tau_{1\%F}(T)} \tag{2}$$

In equation (2), $CCR_{1\%\,F}$ is the constant cooling rate for the formation of 1% ferrite, and $\tau_{1\%\ F}(T)$ is the isothermal time delay required to form 1% ferrite as a function of temperature. A similar equation can be written for the bainitic reaction.

Kim *et al.*[37] calculated CCT curves for different locations in the HAZ of an SA508 reactor pressure vessel steel weld using the model described by Li and coworkers, and their results are shown in Fig. 5. The Ae_3 and Ae_1 temperatures were calculated using commercially available thermodynamic software, and they estimated the austenite grain sizes for their steel according to a generalised equation for grain growth proposed by Leblond and Devaux,[38] namely

$$\begin{aligned} \frac{d}{dt}(zD^a) &= zC\exp\left(-\frac{Q}{RT}\right), \quad \frac{dz}{dt} \geqslant 0 \\ \frac{d}{dt}(zD^a) &= C\exp\left(-\frac{Q}{RT}\right), \quad \frac{dz}{dt} < 0 \end{aligned} \tag{3}$$

where t is time, z is the volume fraction of austenite, D^a is average grain size, and Q is the activation energy for the steel. The significance of grain size variations within the HAZ is evident in Fig. 5 – the predicted proportions of product phases would differ significantly between the two locations under consideration. Note also that transformations within the HAZ of a welded joint are predicted to occur more rapidly than when the same steel has been austenitised at 890°C for 15 min (Fig. 4). Thus, it is evident that if a CCT diagram for the parent plate material is to be used to predict weld microstructures, it is necessary to know the corresponding austenite grain size and account for the different grain sizes that will arise in the HAZ of a welded joint.

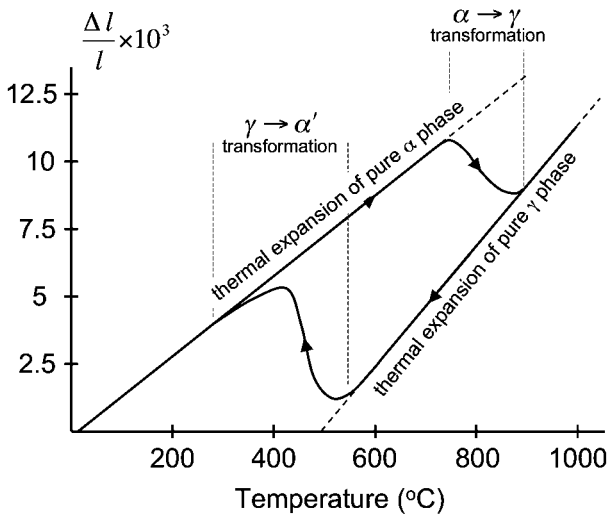

7 Dilatometric diagram of A508 class 3 reactor pressure vessel steel heated at 30 K s^{-1} and cooled at 2 K s^{-1} (Ref. 40)

Transformation effects

The mechanism by which austenite transforms upon cooling can be described as being either reconstructive or displacive.[31] The former mechanism involves the diffusion of all elements, including iron. Allotriomorphic (grain boundary) ferrite, idiomorphic ferrite and pearlite are all products of reconstructive transformations. The only strain that cannot then be cancelled by diffusion is the volume change due to the difference in densities of the parent and product phases – the strain due to reconstructive transformations in steels is therefore an isotropic volume change.

In contrast, displacive transformations typically involve an invariant plane strain shape deformation with a large shear parallel to the invariant plane and a dilatation normal to the plane (the invariant plane is often referred to as the habit plane). They do not involve the diffusion of iron atoms or substitutional solutes. Widmanstätten ferrite, acicular ferrite, bainite and martensite are all products of displacive transformations.[31] Here the movement of iron and substitutional solutes occurs in a coordinated manner, leading to a well defined and reproducible crystallographic relationship between the parent and product phases. It is emphasised that while displacive transformations in steels are associated with a volume change, this change is not isotropic but occurs as a dilatation normal to the habit plane which remains macroscopically undistorted. Furthermore, the volume strain is typically 0·03, which is much smaller than the shear strain which is typically 0·26 (Ref. 39). The different features of reconstructive and displacive transformations are illustrated in Fig. 6.

The volume changes that occur in steels as they are heated and cooled can be inferred from dilatometry, where the change in length of an unloaded specimen is measured as a function of temperature. Figure 7 illustrates such an experiment[40] – the upper straight line represents the expansion of the body centred cubic phase (ferrite, bainite, martensite) and the lower line that of austenite (γ). Data at locations between the upper and lower lines correspond to the co-existence of the parent and product phases. The transformations occurred at

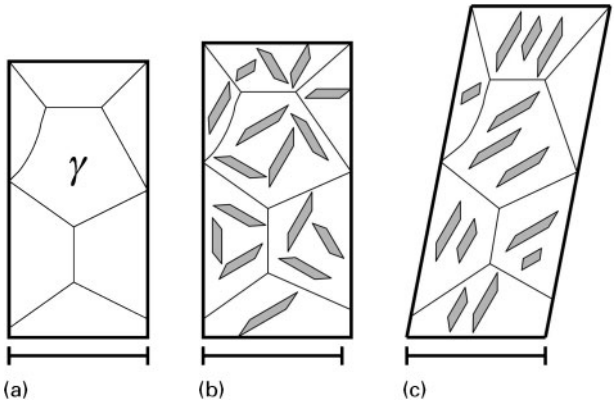

8 Polycrystalline specimen of austenite *a* may transform by displacive mechanism in absence of macroscopic stress to *b* randomly orientated sets of plates or, in presence of macroscopic stress, to *c* sets of plates with orientations that favour compliance with stress

different temperatures upon heating and cooling. The transformation temperature is a function of the cooling rate, steel composition and austenite grain size. The measured coefficient of thermal expansion is larger for austenite ($\sim 23 \times 10^{-6}\ K^{-1}$) than for ferrite ($\sim 15 \times 10^{-6}\ K^{-1}$). As a consequence, the volume change due to transformation is greater during cooling than during heating. The volume expansion due to the transformation of austenite can partly compensate for thermal contraction strains arising as a welded joint cools.[41,42]

Each grain of austenite can in general transform into 24 crystallographic variants of bainite or martensite. When all of these form, the effect on a macroscopic scale is that the shear strains due to the totality of plates average to zero. The volume strain cannot be cancelled in this way since it is always positive with respect to the sample frame, but because of the large number of variants that form, the dilatation observed macroscopically appears isotropic, even though that associated with an individual plate is not (Fig. 6).

The situation changes when a displacive transformation is influenced by external stress because those crystallographic variants whose transformation strain complies with the stress are favoured,[43] as illustrated in Fig. 8. The shear components of the shape deformation then become prominent,[44] all dimensional changes become anisotropic,[45–47] and the material acquires a transformation texture.[48,49] Because the shear strain component is relatively large, there is a much greater potential to exploit the phase change in order to mitigate the residual stresses that develop during the cooling of welds.[50]

Variant selection has been reported in simulated weld specimens by Bhadeshia *et al.*,[45] who showed that the presence of stresses well below the yield stress led to the preferential selection of crystallographic variants in a bainitic pressure vessel steel. These workers also observed that a non-random austenite texture aids the development of a transformation texture and hence anisotropic strains. As emphasised previously, the large shear component of the invariant plane strain deformation, as illustrated in Fig. 6, would also suggest that large reductions in stress can be achieved through the variant selection mechanism, until the point is reached where the transformation is exhausted.

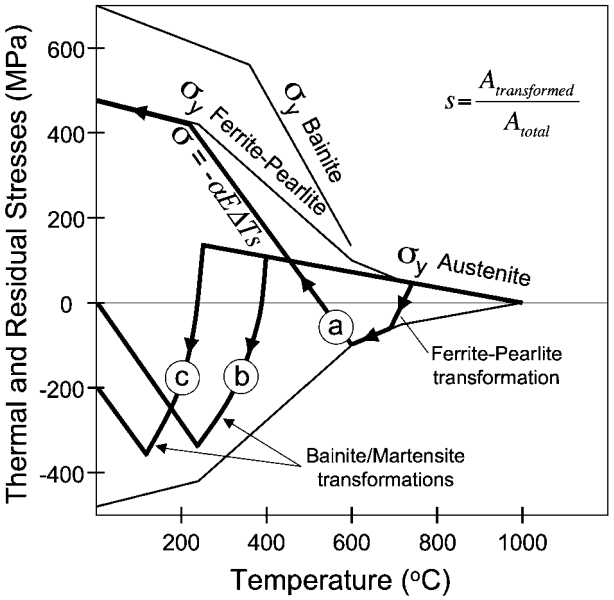

9 Schematic representation of axial stress development in uniaxially constrained samples during cooling for *a* ferritic pearlitic, *b* bainitic and *c* martensitic steels:[53] parameter *s* is fraction of cross-section that has transformed

Jones and Alberry conducted experiments that illustrate the effects of phase transformations on residual stress development in steels.[51,52] They measured the stresses that were developed in tensile specimens whose ends were rigidly fixed at a high temperature in the austenite phase field, and then allowed to cool, for three cases: non-transforming austenitic, bainitic and martensitic steels. A schematic representation of the development of residual stresses in experiments of this type is given in Fig. 9 for three different transformation events.[53]

Before the commencement of a transformation, all of the constrained samples would develop stresses comparable to the yield strength of austenite. This is to be expected because, for an austenite thermal expansion coefficient of $23 \times 10^{-6}\ K^{-1}$ and a modulus of 200 GPa, contraction stresses in excess of 400 MPa would develop for every 100°C of cooling.[39] These are too large to be accommodated elastically, causing the sample to relax by plastic deformation down to the yield strength. However, the stresses in each sample start to diminish towards zero at the beginning of the respective transformations to ferrite pearlite (~700°C) bainite (~400°C) and martensite (~250°C). During this stage the transformation strains overwhelm the effect of thermal contraction as the temperature decreases. However, once the austenite is exhausted, continued thermal contraction causes once again the accumulation of stress.

There are two further features which are noteworthy. First, because the martensite transformation occurs at a lower temperature than the bainite and ferrite pearlite transformations, the residual stress left at ambient temperature is much smaller. This is because there is a smaller range between the martensite finish and ambient temperatures, thus minimising the regime over which thermal contraction alone is active once the transformation is completed. It clearly is an advantage to engineer the transformation finish temperature to be close to the ambient temperature.

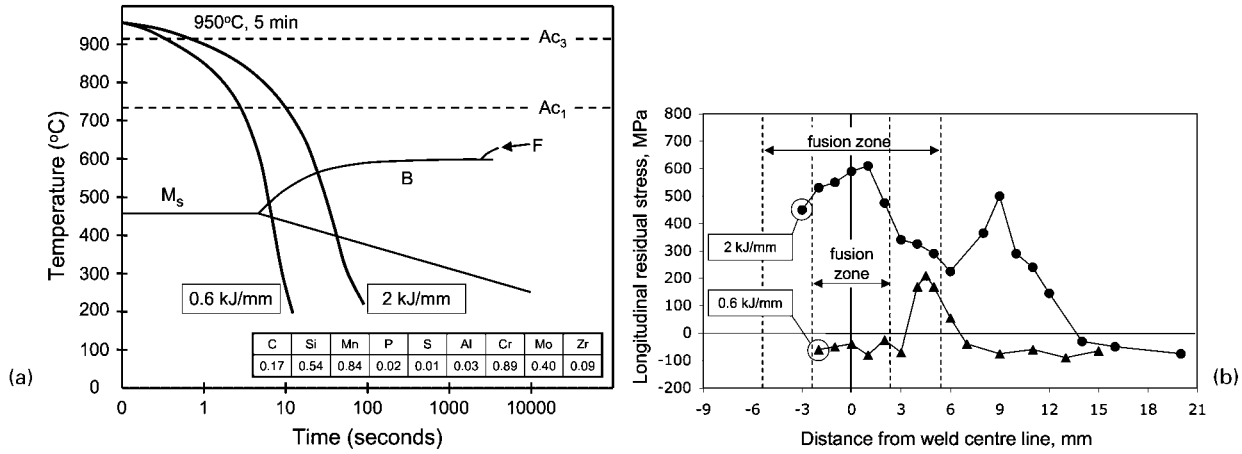

10 Effects of weld heat input on *a* transformation temperature and *b* longitudinal residual stresses:[53] steel composition is given in wt-% in *a*

A second observation is that because the martensite transformation commences at a lower temperature than is the case for bainite, the stress experienced by the martensite at its initiation is greater. This will lead to a greater degree of variant selection, i.e., to favour those variants which comply with the stress. It follows that the shear component of the shape deformation for displacive transformations becomes much more prominent as the transformation temperature decreases, leading to a greater reduction in stress and the possibility of overshooting into compression. In summary, a second advantage of promoting transformation to lower temperatures is that it then occurs under the influence of a larger accumulated stress, thus permitting greater variant selection and exploitation of the transformation strain. With ideal variant selection it is possible to obtain an elongation due to transformation alone of some 15%.[50]

Residual stresses

Residual stresses can be classified according to the length scale over which they self-equilibrate in the plane normal to which they act.[1] Macrostresses (type I) occur on scales in which the material can be considered as a continuum, and span distances that approach (but are not greater than) a characteristic dimension of the structure. For example, Bouchard and Withers[54] describe the case of a welded thick walled pipe where, from a residual stress standpoint, one characteristic distance might be the length of the pipe, another might be its wall thickness and a third might correspond to the dimensions of individual beads within the welded joint. Type I stresses that act over one of these characteristic dimensions could be categorised as either long range, medium range or short range respectively. In addition, type II stresses are usually present in polycrystalline or multiphase materials as intergranular stresses, whereas type III stresses arise within individual grains and are associated with point defects and dislocations.[54] In integrity assessments on power plant welds, the focus must be (and usually is) on type I stresses. The role of the types II and III stresses becomes prominent primarily when designing materials – as a variation of stress on a microstructural scale is likely to lead to localised corrosion attack in appropriate circumstances.

The choice of welding parameters can influence the distribution of residual stress in ferritic welds since, together with the joint thickness and configuration; they largely determine the cooling rates that are experienced across the joint. This was demonstrated by Nitschke-Pagel and Wohlfahrt,[53] who presented residual stress distributions for two gas tungsten arc steel welds made with different heat inputs. The composition of their steel is given in Fig. 10*a*, which also shows recorded cooling curves for each weld plotted against the corresponding CCT diagram. The variation in longitudinal stress with distance from the weld centreline is plotted for each weld in Fig. 10*b*. It can be seen that the selection of a lower heat input led to a lower transformation temperature, which would have reduced the scope for contraction stresses to generate after the transformation was exhausted. Consequently, for the low heat input weld the longitudinal residual stresses are slightly compressive near to the weld centreline, in contrast to the high tensile stresses that were generated in the high heat input weld.

The pronounced effect of transformation temperature on welding residual stresses has stimulated efforts to design filler metals with optimised transformation temperatures. There is a philosophical difference to note in this approach. Rather than requiring tight control over welding parameters in order to achieve a low transformation temperature, the composition of the filler metal is carefully selected so that, in the fusion zone, the ferrite pearlite and bainite transformations are avoided at cooling rates that are likely to be experienced in a welded joint. Thus, while the CCT curve is further to the right (longer times) for the ferrite pearlite and bainite transformations, the martensite transformation also occurs over a desired temperature range. Ohta *et al.*[55,56] and Wang *et al.*,[57] for example, have proposed welding electrodes that achieve martensite start temperatures at or just under 200°C and martensite finish temperatures close to room temperature, and they have achieved near zero or compressive residual stresses in the fusion zones of their welds.

The restraint on an assembly during welding must naturally influence the nature and extent of residual stresses. Price *et al.*[58] studied single weld beads deposited using gas metal arc welding (GMAW) on to 12 mm thick low carbon steel plates. In one case the plate was

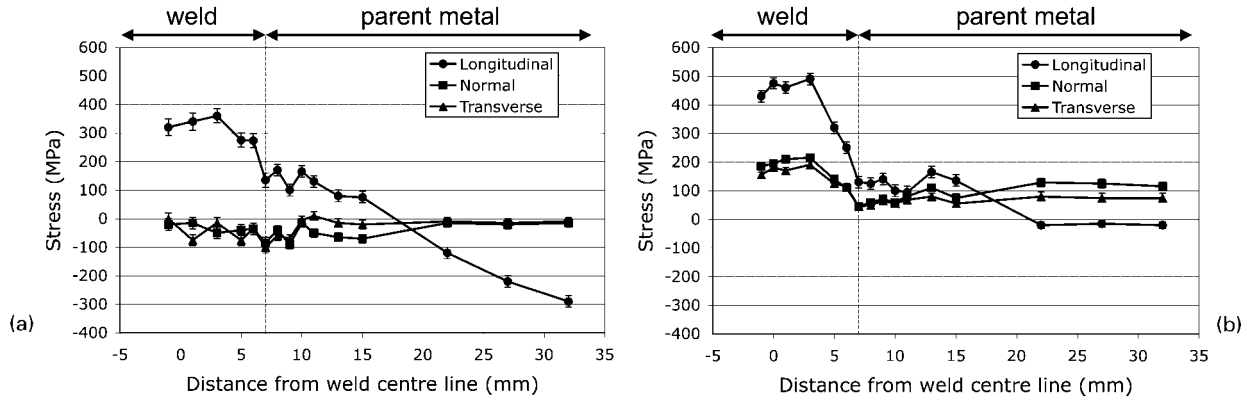

11 Effect of restraint on residual stresses measured 1·5 mm below surface by neutron diffraction in *a* unrestrained and *b* restrained GMAW single bead welds deposited on 12 mm thick low carbon steel plates[58]

not restrained during welding whereas in the other it was made more rigid by tack welding to a very thick steel substrate. After removal from the restraining plate, stresses were measured 1·5 mm below the plate surface, at different distances from the weld centreline, by neutron diffraction – the results are illustrated in Fig. 11. For the unrestrained plate, the longitudinal tensile weld stresses of approximately 350–360 MPa are ~25% higher than the estimated yield strength of the material when measured in monotonic tension (285 MPa). The peak stresses in the restrained case are more tensile overall, being closer to 500 MPa in the weld and less compressive in the parent plate, with a corresponding increase in the hydrostatic component of stress.

At present there appears to be a dearth of data relating to bulk residual stresses in multipass ferritic steel welds. However, Smith *et al.*[14] have made measurements down the weld centreline in a ferritic steel pipe with a wall thickness of 84 mm using the deep hole drilling method. The hoop and axial components of stress are plotted as a function of distance from the outer surface of the pipe in Fig. 12, for both the as welded and post-weld heat treated (PWHT) conditions. Before PWHT, the maximum tensile stresses were measured in the hoop direction, midway through the wall thickness. Apart from a small region of compression near the inner surface of the pipe, the hoop stresses were entirely tensile. While the axial stresses were compressive near each surface, they were also tensile across the majority of the pipe wall. Post-weld heat treatment resulted in significant relaxation of both the tensile and compressive residual stresses across the pipe wall. Interestingly, despite the fact that the radial stress was not measured here, it seems plausible that only the deviatoric component of stress, and not the hydrostatic component, was relieved by PWHT. (Hydrostatic residual stresses may have accumulated during welding once a sufficient number of passes had been deposited to provide a high level of restraint for later passes, i.e. at a certain distance from the inner surface of the pipe.) It is possible that the deviatoric component of stress is relieved during PWHT by dislocation creep, whereas the hydrostatic component of stress may only relieved by longer term mechanisms involving diffusion and grain boundary sliding, as has been suggested by Kimmins and Smith.[59] Indeed, there is a great need to understand how hydrostatic stresses evolve when subjected to thermal aging, either in the context of PWHT or creep during service. This has recently inspired efforts to design samples for material testing in which triaxial stresses can be generated across significant volumes of the specimen.[60]

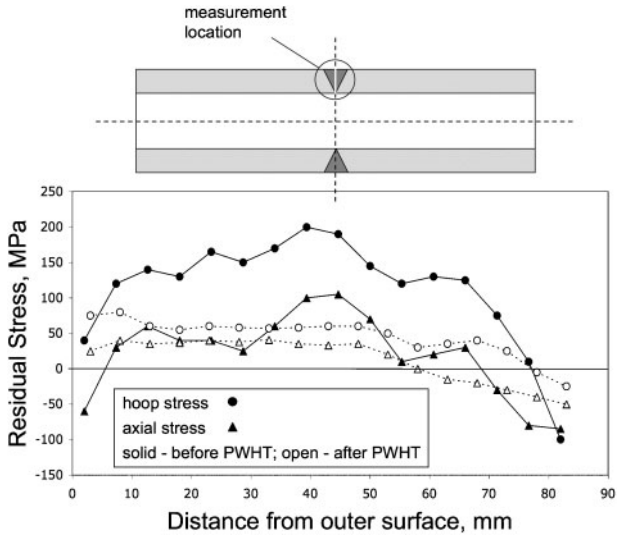

12 Through wall axial and hoop residual stress measurements in ferritic steel pipe girth weld[14]

Modelling challenges

Within the community concerned with modelling of residual stresses, fusion welding is often considered to involve a combination of thermal, metallurgical and mechanical processes. It is common and computationally efficient to use a one way coupled approach,[61] i.e. accounting for thermal history in a mechanical analysis while ignoring the effect of mechanical work in a thermal analysis. Complex arc and weld pool phenomena are generally not considered and instead pragmatic models for the welding heat source are implemented. Gas tungsten arcs, for example, are often represented by Gaussian heat distributions such as the double ellipsoid model proposed by Goldak *et al.*,[62] or a combination of surface flux and body flux.[63] The characteristic parameters required by such models are usually obtained using a calibration procedure whereby, for a well defined test case, the best agreement is sought between either the predicted and measured location of the fusion surface, or the predicted and measured thermal excursion

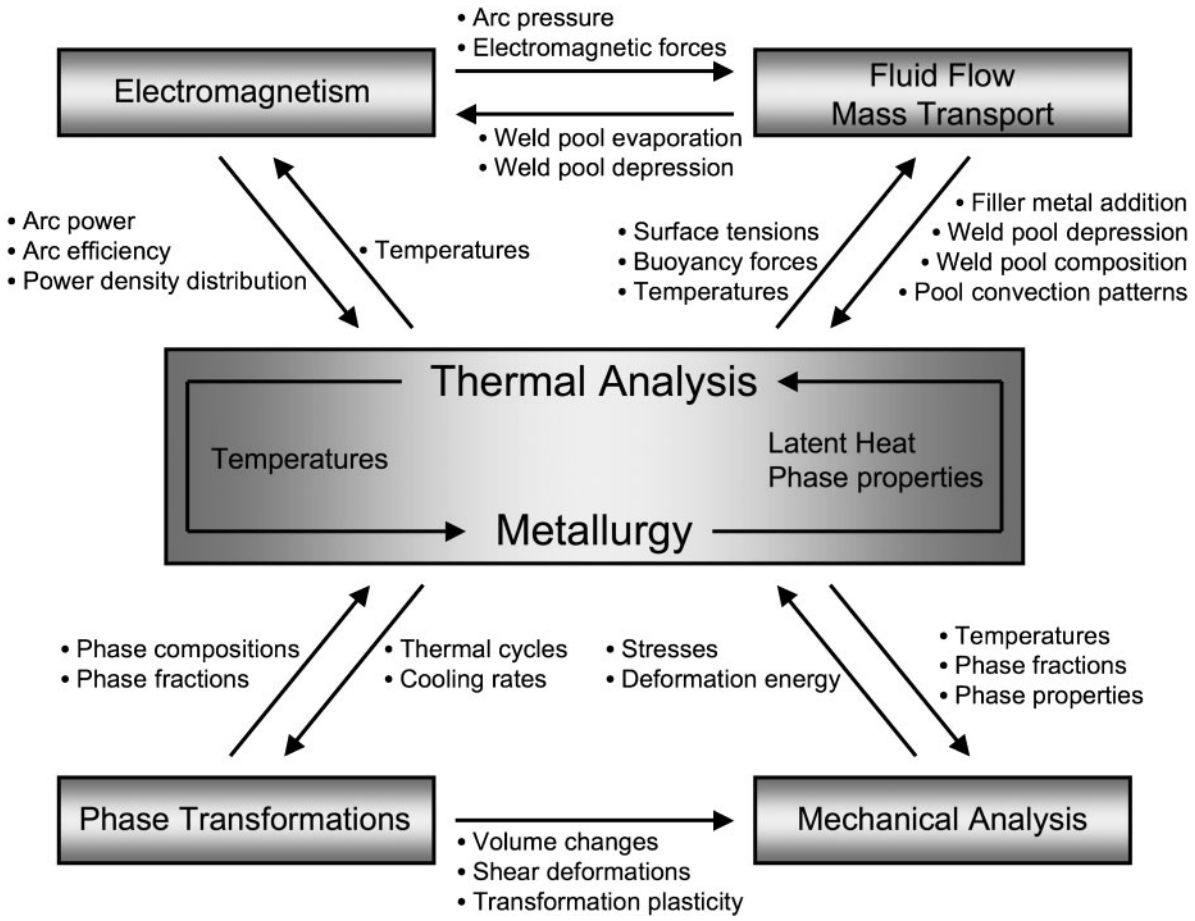

13 Processes and interactions that arise in arc welding of ferritic steels: engineering integrity assessments currently focus on the lower half of the diagram

recorded at one or more locations. Indeed, the complex nature of welding processes necessitates a significant number of simplifying assumptions, and in many circumstances these need not be obstacles to the attainment of acceptable results.[64]

In addition to thermal, metallurgical and mechanical processes, the arc and weld pool are host to complex electromagnetic processes, as well as fluid and mass transport. Details of these physical processes can be obtained elsewhere,[65,66] and are only briefly mentioned here. It is important to mention, however, that these processes do have implications for residual stress development. The divergence of current within the welding arc, for example, generates a plasma jet that places a downward pressure, referred to as arc pressure, on the weld pool. The weld pool has a free surface that may distort under the influence of arc pressure, and any changes in weld pool shape can lead to significant changes in the profile of the fusion line. Furthermore, the temperature gradients (and compositional gradients) that arise within the weld pool give rise to associated surface tension gradients and buoyancy forces which, together with an electromagnetic force, drive convection within the weld pool. It is well established that weld pool convection patterns can have dramatic effects on the profile of the fusion line.[65,66] Given that the shape of the fusion surface is influenced by such complex phenomena, it is not reasonable to expect approximate heat source models to accurately reproduce the shape of the fusion surface and near weld temperature fields for all test cases. As such, care needs to be taken when using the fusion surfaces as a basis for calibrating idealised heat source models. There are in fact hybrid models which are better at modelling realistic weld pool shapes by using neural networks which are constrained by the physics described above.[67]

There has been significant progress in recent years towards understanding and modelling complex arc and weld pool phenomena,[68,69] but this progress has generally not permeated through to calculations of residual stress development. If arc and weld pool phenomena were to be integrated into models for residual stress, the complex nature of the physical processes and their interactions might be represented schematically as in Fig. 13. As might be expected, many researchers and engineers who are concerned with residual stress development focus primarily on the metallurgical and mechanical processes that take place during welding (i.e. those in the bottom half of Fig. 13). It may be computationally prohibitive to attempt to account for all of the phenomena shown in Fig. 13 in engineering integrity assessments. However, within academic and research communities in particular, it may prove fruitful to explore integrated modelling approaches in order to establish domains in which simplifying assumptions can be made with minimal losses in accuracy and, simultaneously, identify the physical processes that do need to be incorporated in to residual stress models for engineering integrity assessments in the future.

With respect to metallurgical processes, complexity is introduced by solid state phase transformations and the

thermal cycling that takes place in multipass ferritic power plant welds. However, the modelling of microstructural evolution was greatly assisted by a mathematical formalism due to Leblond and Devaux[38] who proposed evolution equations for transformations of the following form

$$\frac{dz}{dt} = \frac{z_{eq}(T) - z}{\tau(T)} \quad (4)$$

where z, for example, is the proportion of austenite, t is time, z_{eq} is the equilibrium proportion of austenite, τ is the time constant for the transformation and T is the temperature. The equation basically assumes that the rate of reaction is proportional to the deviation from equilibrium and therefore asymptotically achieves the equilibrium fraction as time increases. The model can cope with the case where the equilibrium fraction is not unity, i.e. situations in which $z_{eq}<1$, and can account for hysteresis (Fig. 7) where the transformation on cooling occurs over a different temperature range than for the reverse transformation on heating. Sluggish reaction kinetics can also be accommodated by redefining the equilibrium proportion of a phase such as ferrite, for example, to be the proportion that is achieved under very slow cooling conditions. Finally, the effects of austenite grain size can be accounted for if the evolution equations are coupled with an equation for average austenite grain size, such as equation (3).[38]

The Leblond and Devaux model requires experimental data in the form of a CCT diagram for the steel of interest in order to derive the fitting constants. The authors have seen though that Kirkaldy and Venugopalan[32] and later Li *et al.*[33] have proposed models that predict CCT diagrams for steels. Furthermore, the initial model proposed by Kirkaldy has been shown to make reasonable predictions for HAZ microstructures in welds.[70,71] Thus, a framework exists for the prediction of phase transformations during multipass welding. It is important, however, to bear in mind that these models do not account for any microstructural changes that might be associated with the tempering effects of subsequent weld passes. It might also be useful, on a given steel, to conduct experiments that establish whether there are likely to be any significant changes in the CCT diagram from one thermal cycle to the next.

The components of strain in mechanical analyses have been described by Lindgren,[72] and can be summarised as follows

$$\varepsilon = \varepsilon_e + \varepsilon_p + \varepsilon_{vp} + \varepsilon_c + \varepsilon_{th} + \varepsilon_{tp} \quad (5)$$

where ε denotes strain and the subscripts e, p, vp, c, th, tp denote elastic, plastic, viscoplastic, creep, thermal and transformation plasticity respectively. Among these, the only component that is somewhat unique to ferritic steels, at least in the context of power plant components, is the strain associated with transformation plasticity. This component arises due to the volume and shear strains associated with austenite to α' transformations, as well as the extent to which variant selection takes place under the action of stress in the event of a bainitic or martensitic transformation. There is also a contribution associated with hard product phases, such as martensite, inducing plasticity in the softer parent phase (austenite) as a transformation proceeds. To date, it appears that variant selection has not been incorporated in to models for welding residual stresses. The fact that the shear component of the deformation during an austenite to bainite/martensite transformation is much greater than the dilatational component would suggest that it is important to incorporate variant selection in to residual stress models. However, in the first instance there appears to be a need to characterise the extent to which variant selection occurs in welded joints. To perform this would also require additional information on the austenite grain structure – grain size data would not be sufficient. A knowledge of the crystallographic texture of the austenite is also essential since it influences the transformation texture and hence the transformation strains. Effects of variant selection on the generation of compressive residual stresses in welds made with low transformation temperature filler metals would also appear to provide interesting avenues for investigation.

The thermomechanical cycling that occurs during multipass welding presents challenges due to the simultaneous occurrence of deformation and annealing. Strain cycling and the Bauschinger effect are usually accounted for through the application of hardening models such as isotropic or kinematic hardening,[73,74] or a mixed hardening model. Simple methods of accounting for annealing effects include the resetting of plastic strain to zero upon exceeding a certain temperature. However, such an approach is not representative of reality. Annealing effects present challenges in weld modelling because they change the effective accumulated plastic strain, as defined in equation (5), in addition to altering the microstructure and mechanical properties. At present there is a need for developmental work on annealing models in ferritic welds. A related issue is the occurrence of strain saturation effects and the possibility for 'block dumping' of weld beads. For example, in a multipass weld with more than 50 weld passes, it is extremely useful to know whether it is necessary to model the deposition of every pass individually, or whether the strain cycling and annealing effects saturate after a small number of passes. If it can be established that saturation occurs after only a few beads have been deposited, then substantial efficiencies in modelling can be achieved by introducing subsequent beads in blocks (or groups).

The need to account for the shape of individual weld beads, together with the effects of annealing and variant selection in models for residual stress development in multipass ferritic welds was recently reported by Deng and Murakawa.[75] They considered four test cases when they modelled the effects of the martensite transformation on welding residual stresses in a 9Cr–1Mo steel pipe. The cases included: no change in volume or phase dependent yield stress; changes in volume only; changes in yield stress only; and changes in both volume and yield stress. They also compared their predictions with measured surface stresses. The predicted and measured hoop stresses on the outer surface of the pipe are shown for the four modelling cases in Fig. 14. It can be seen that compressive stresses are predicted in parts of the weld metal for the cases that considered volume changes. However, the best agreement was observed when only volume changes were considered. They reasoned that in their models, the changes in yield stress upon transformation were being over estimated due to the annealing

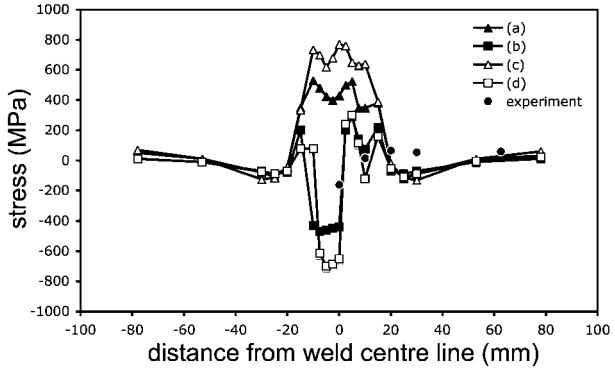

a no changes in volume or phase dependent yield stress; *b* changes in volume only; *c* changes in yield stress only; *d* changes in both volume and yield stress[75]

14 Comparison between measured and predicted residual stresses in welded 9Cr–1Mo steel for four test cases

that occurs upon deposition of subsequent weld passes. Although both models that considered the effects of volume changes achieved reasonable agreement with measurements, Deng and Murakawa suggested that further improvements could be achieved if the shapes of individual weld beads were accounted for accurately, and effects such as those due to transformation plasticity were also incorporated.

Suggestions for future work

In summary, progress continues to be made in our understanding of welding residual stresses in ferritic power plant steels. There remain exciting and challenging opportunities for future work. Some areas that deserve particular mention include the following parts.

1. Integrated modelling approaches: there is a need to integrate models for complex arc, weld pool and solidification phenomena in to a modelling framework for residual stress development. This will require both interdisciplinary expertise and computational resources. The reward would be tangible in terms of the understanding of the origin of residual stresses and in identifying the controlling aspects of the problem.

2. Variant selection: variant selection is not yet incorporated into models for welding residual stresses. This is anomalous since variant selection in bainitic and martensitic transformations may affect residual stress development to a greater extent than any volume changes, since the shear component of the associated deformation is significantly larger than the dilatational component. A viable theory for the extent of variant selection must depend on the balance between the mechanical and chemical driving forces for transformation. Variant selection is expected to be strong when the ratio of the mechanical to chemical driving force is large. Experimental work is also required to confirm the extent to which austenite texture and variant selection during bainitic and martensitic transformations affect residual stresses in ferritic steel welds.

3. Thermomechanical cycling effects on transformations: transformations in steels depend not only on the composition, austenite grain size and cooling rate but also on stress and thermal history. Welding gives rise to many possible combinations of thermomechanical cycles and, as such, it is conceivable that the CCT diagram and transformation behaviour may change from one weld pass to the next. Thus, the study of the response of steels to thermomechanical cycling appears to be an important and exciting area in which to conduct research.

4. Annealing models: development is needed on models for the effects of annealing in multipass welds. Current approaches tend to underestimate the annealing that takes place due to the thermal cycles associated with subsequent weld passes.

5. Implications for weld design: it is hoped that advances in our understanding of residual stress development will ultimately translate to improvements in joining technology and weld design. Ongoing work is required to understand how the mechanical and transformation properties of filler metals, the selection of welding parameters such as the preheat temperature, the pass sequence and the joint configuration can all be optimised with respect to residual stresses and weld integrity.

Acknowledgements

The authors would like to acknowledge helpful discussions with Dr Hui Dai and Dr Mark Turski at the University of Manchester. JAF is also grateful for support from Roll-Royce Naval Marine.

References

1. P. J. Withers and H. K. D. H. Bhadeshia: 'Residual stress part 1 – measurement techniques', *Mater. Sci. Technol.*, 2001, **17**, (4), 355–365.
2. P. J. Withers and H. K. D. H. Bhadeshia: 'Residual stress part 2 – nature and origins', *Mater. Sci. Technol.*, 2001, **17**, (4), 366–375.
3. D. Radaj: 'Heat effects of welding – temperature field, residual stress, distortion', 1–18; 1992, Berlin Heidelberg, Springer-Verlag.
4. X. H. Cheng, J. W. Fisher, H. J. Prask, T. Gnaupel-Herold, B. T. Yen and S. Roy: 'Residual stress modification by post-weld treatment and its beneficial effect on fatigue strength of welded structures', *Int. J. Fatig.*, 2003, **25**, (9–11), 1259–1269.
5. W. Fricke: 'Effects of residual stresses on the fatigue behaviour of welded steel structures', *Mater. Werkstofftechn.*, 2005, **36**, (11), 642–649.
6. D. J. Hornbach and P. S. Prevey: 'The effect of prior cold work on tensile residual stress development in nuclear weldments', *J. Press. Vessel Technol.*, 2002, **124**, (3), 359–365.
7. D. P. G. Lidbury: 'The significance of residual stresses in relation to the integrity of LWR pressure vessels', *Int. J. Press Vessels Piping*, 1984, **17**, (4), 197–328.
8. D. T. Read: 'Measurement of applied j-integral produced by residual-stress', *Eng. Fract. Mech.*, 1989, **32**, (1), 147–153.
9. M. Turski, A. H. Sherry, P. J. Bouchard and P. J. Withers: 'Residual stress driven creep cracking in type 316 stainless steel', *J. Neutron Res.*, 2004, **12**, (1–3), 45–49.
10. P. J. Bouchard, P. J. Withers, S. A. McDonald and R. K. Heenan: 'Quantification of creep cavitation damage around a crack in a stainless steel pressure vessel', *Acta Mater.*, 2004, **52**, (1), 23–34.
11. R. A. Ainsworth, J. K. Sharples and S. D. Smith: 'Effects of residual stresses on fracture behaviour – experimental results and assessment methods', *J. Strain Anal. Eng. Design*, 2000, **35**, (4), 307–316.
12. R. A. Ainsworth: 'R5 procedures for assessing structural integrity of components under creep and creep-fatigue conditions', *Int. Mater. Rev.*, 2006, **51**, (2), 107–126.
13. Y. Lei, N. P. O'Dowd and G. A. Webster: 'Fracture mechanics analysis of a crack in a residual stress field', *Int. J. Fract.*, 2000, **106**, (3), 195–216.
14. D. J. Smith, P. J. Bouchard and D. George: 'Measurement and prediction of residual stresses in thick-section steel welds', *J. Strain Anal. Eng. Design*, 2000, **35**, (4), 287–305.
15. P. Duranton, J. Devaux, V. Robin, P. Gilles and J. M. Bergheau: '3D modelling of multipass welding of a 316L stainless steel pipe', *J. Mater. Process. Technol.*, 2004, **153–154**, 457–463.

16. C. D. Elcoate, R. J. Dennis, P. J. Bouchard and M. C. Smith: 'Three dimensional multi-pass repair weld simulations', *Int. J. Press. Vessels Piping*, 2005, **82**, (4), 244–257.
17. R. Kohno and S. B. Jones: 'An initial study of arc energy and thermal cycles in the submerged arc welding of steel', Technical report 81/1978/PE, The Welding Institute, Abington, Cambridge, England, 1978.
18. S. L. Mannan and K. Laha: 'Creep behaviour of Cr–Mo steel weldments', *Trans. Ind. Inst. Met.*, 1996, **49**, (4), 303–320.
19. J. A. Francis, W. Mazur and H. K. D. H. Bhadeshia: 'Type IV cracking in ferritic power plant steels', *Mater. Sci. Technol.*, 2006, **22**, (12), 1387–1395.
20. V. Karthik, K. V. Kasiviswanathan, K. Laha and B. Raj: 'Determination of gradients in mechanical properties of 2·25Cr–1Mo weldments using shear-punch tests', *Weld. J.*, 2002, **81**, (12), 265S–272S.
21. J. F. Lancaster: 'Metallurgy of welding', 6th edn, 211–309; 1999, Abington, Cambridge, Abington Publishing.
22. R. K. Nanstad, D. E. McCabe, M. A. Sokolov, C. A. English and S. R. Ortner: 'Comparison of effects of thermal aging, irradiation, and thermal annealing on the propensity for temper embrittlement on an RPV submerged-arc weld HAZ', ORNL Letter report ORNL/NRC/LTR-01/07, Oak Ridge National Laboratory, December 2001.
23. S. Issler, A. Klenk, A. A. Shibli and J. A. Williams: 'Weld repair of ferritic welded materials for high temperature application', *Int. Mater. Rev.*, 2004, **49**, (5), 299–324.
24. K. S. Kweon, J. H. Kim, J. H. Hong and C. H. Lee: 'Microstructure and toughness of intercritically reheated heat affected zone in reactor pressure vessel steel weld', *Sci. Technol. Weld. Join.*, 2000, **5**, (3), 161–167.
25. M. Hamada: 'Control of strength and toughness at the heat affected zone', *Weld. Int.*, 2003, **17**, (4), 265–270.
26. G. M. Reddy, T. Mohandas and D. S. Sarma: 'Cold cracking studies on low alloy steel weldments: effect of filler metal composition', *Sci. Technol. Weld. Join.*, 2003, **8**, (6), 407–414.
27. J. Onoro: 'Weld metal microstructure analysis of 9–12% Cr steels', *Int. J. Press. Vessels Piping*, 2006, **83**, 540–545.
28. A. C. Hunt, A. O. Kluken and G. R. Edwards: 'Heat input and dilution effects in microalloyed steel weld metals', *Weld. J.*, 1994, **73**, (1), S9–S15.
29. K. Easterling: 'Introduction to the physical metallurgy of welding', 2nd edn, 1–54; 1992, Oxford, Butterworth Heinemann.
30. K. Suzuki, I. Kurihara, T. Sasaki, Y. Koyoma and Y. Tanaka: 'Application of high strength MnMoNi steel to pressure vessels for nuclear power plant', *Nuclear Eng. Design*, 2001; **206**, 261–278.
31. H. K. D. H. Bhadeshia: 'Steels – microstructure and properties', 3rd edn; 2006, Oxford, Elsevier.
32. J. S. Kirkaldy and D. Venugopalan: 'Prediction of microstructure and hardenability in low alloy steels', in 'Phase transformations in ferrous alloys', (eds. A. R. Marder and J. I. Goldstein), 125–148; 1984, New York, AIME.
33. M. V. Li, D. V. Niebuhr, L. L. Meekisho and D. G. Atteridge: 'A computational model for the prediction of steel hardenability', *Metall. Mater. Trans. B*, 1998, **29B**, (3), 661–672.
34. C. Zener: 'Kinetics of the decomposition of austenite', *Trans. AIME*, 1946, **167**, 550–583.
35. M. Hillert: 'The role of interfacial energy during solid state phase transformations', *Jernkont. Ann.*, 1957, **141**, 557–585.
36. K. W. Andrews: *J. Iron Steel Inst.*, 1969, **203**, 721–727.
37. J.-S. Kim, S.-H. Lee and T.-E. Jin: 'Fatigue evaluation of dissimilar welds on nuclear components', Proc. 17th Int. Conf. on 'Structural mechanics in reactor technology' (SMiRT 17), Prague, Czech Republic, August 2003, International Association for Structural Mechanics in Reactor Technology, Paper D03-2.
38. J. B. Leblond and J. Devaux: 'A new kinetic model for anisothermal metallurgical transformations in steels including effect of austenite grain size', *Acta Metall.*, 1984, **32**, (1), 137–146.
39. H. K. D. H. Bhadeshia: 'Developments in martensitic and bainitic steels: role of the shape deformation', *Mater. Sci. Eng. A*, 2004, **A378**, (1–2), 34–39.
40. J. B. Leblond, G. Mottet and J. C. Devaux: 'A theoretical and numerical approach to the plastic behaviour of steels during phase transformations', *J. Mech. Phys. Solids*, 1986, **34**, (4), 395–409.
41. G. W. Greenwood and R. H. Johnson: *Proc. Royal Soc.*, 1965, **238**, 403–422.
42. R. H. Johnson and G. W. Grenwood: *Nature*, 1962, **195**, 138–139.
43. J. R. Patel and M. Cohen: *Acta Metall.*, 1953, **1**, 531–538.
44. C. L. Magee: 'Phase transformations', (eds. V. F. Zackay and H. I. Aaronson), 115–156; 1970, Metals Park, OH, ASM.
45. H. K. D. H. Bhadeshia, S. A. David, J. M. Vitek and R. W. Reed: 'Stress induced transformation to bainite in Fe–Cr–Mo–C pressure vessel steel', *Mater. Sci. Technol.*, 1991, **7**, (8), 686–698.
46. P. H. Shipway and H. K. D. H. Bhadeshia: 'The effect of small stresses on the kinetics of the bainite transformation', *Mater. Sci. Eng. A*, 1995, **A201**, 143–149.
47. A. Matsuzaki, H. K. D. H. Bhadeshia and H. Harada: *Acta Metall. Mater.*, 1994, **42**, 1081–1090.
48. N. Gey, B. Petit and M. Humbert: *Metall. Mater. Trans. A*, 2005, **36A**, (12), 3291–3299.
49. S. Kundu and H. K. D. H. Bhadeshia: *Scr. Mater.*, 2006, **55**, 779–781.
50. H. K. D. H. Bhadeshia: *ISIJ Int.,* 2002, **42**, 1059–1060.
51. W. K. C. Jones and P. J. Alberry: in 'Ferritic steels for fast reactor steam generators', 1–4; 1977, London, British Nuclear Engineering Society.
52. W. K. C. Jones and P. J. Alberry: in 'Residual stresses in welded constructions', 1977, Cambridge, The Welding Institute.
53. T. Nitschke-Pagel and H. Wohlfahrt: 'Residual stresses in welded joints – sources and consequences', *Mater. Sci. Forum*, 2002, **404–407**, 215–224.
54. P. J. Pouchard and P. J. Withers: 'The appropriateness of residual stress length scales in structural integrity', *J. Neutr. Res.*, 2004, **12**, (1–3), 81–91.
55. A. Ohta, N. Suzuki, Y. Maeda, K. Hiraoka and T. Nakamura: 'Superior fatigue crack growth properties in newly developed weld metal', *Int. J. Fatig.*, 1999, **21**, S113–S118.
56. A. Ohta, K. Matsuoka, N. T. Nguyen, Y. Maeda and N. Suzuki: 'Fatigue strength improvement of lap joints of thin steel plate using low-transformation-temperature welding wire', *Weld. J.*, 2003, **82**, (4), 78S–83S.
57. W. X. Wang, L. X. Huo, Y. F. Zhang, D. P. Wang and H. Y. Jing: 'New developed welding electrode for improving the fatigue strength of welded joints', *J. Mater. Sci. Technol.*, 2002, **18**, (6), 527–531.
58. J. W. H. Price, A. Paradowska, S. Joshi and T. Finlayson: 'Residual stresses measurement by neutron diffraction and theoretical estimation in a single weld bead', *Int. J. Press. Vessels Piping*, 2006, **83**, 381–387.
59. S. T. Kimmins and D. J. Smith: *J. Strain Anal.*, 1998, **33**, (3), 195–206.
60. S. Hossain, C. E. Truman, D. J. Smith and M. R. Daymond: 'Application of quenching to create highly triaxial residual stresses in type 316H stainless steels', *Int. J. Mech. Sci.*, 2006, **48**, 235–243.
61. R. J. Dennis and N. A. Leggatt: 'Optimisation of weld modelling techniques, bead-on-plate analysis', Proc. ASME PVP2006, Vancouver, Canada, July 2006, ASME.
62. J. Goldak, A. Chakravarti and M. Bibby: 'A new finite-element model for welding heat-sources', *Metall. Trans. B*, 1984, **15B**, (2), 299–305.
63. J. K. Hong, C. L. Tsai and P. Dong: 'Assessment of numerical procedures for residual stress analysis of multipass welds', *Weld. J.*, 1998, **77**, (9), 372S–382S.
64. P. Dong and K. Hong: 'Recommendations for determining residual stresses in fitness for service assessments', WRC Bulletin 476, New York, November 2002.
65. T. Zacharia, J. M. Vitek, J. A. Goldak, T. A. Debroy, M. Rappaz and H. K. D. H. Bhadeshia: 'Modelling of fundamental phenomena in welds', *Model. Simul. Mater. Sci. Eng.*, 1995, **3**, 265–288.
66. T. Debroy and S. A. David: 'Physical processes in fusion welding', *Rev. Modern Phys.*, 1995, **67**, (1), 85–112.
67. S. Mishra and T. Debroy: 'A genetic algorithm and gradient-descent-based neural network with the predictive power of a heat and fluid flow model for welding', *Weld. J.*, 2006, **85**, (11), 231s–242s.
68. A. Kumar and T. Debroy: 'Calculation of three-dimensional electromagnetic force field during arc welding', *J. Appl. Phys.*, 2003, **94**, (2), 1267–1277.
69. S. A. David, S. S. Babu and J. M. Vitek: 'Recent advances in modelling and characterisation of weld microstructures', *Sci. Technol. Weld. Join.*, 2001, **6**, (6), 341–346.
70. D. F. Watt, L. Coon, M. Bibby, J. Goldak and C. Henwood: 'An algorithm for modeling microstructural development in weld heat-affected zones: part A – reaction kinetics', *Acta Metall.*, 1988, **36**, (11), 3029–3035.
71. C. Henwood, M. Bibby, J. Goldak and D. Watt: 'Coupled transient heat transfer-microstructure weld computations: part B', *Acta Metall.*, 1988, **36**, (11), 3037–3046.

72. L.-E. Lindgren: 'Finite element modeling and simulation of welding part 2: improved material modeling', *J. Therm. Stress.*, 2001, **24**, 195–231.
73. M. Preuss, J. Pang, P. J. Withers and G. J. Baxter: 'Inertia welding nickel-based superalloy: metallurgical development', *Metall. Mater. Trans. A*, 2002, **33A**, (10), 3215–3225.
74. M. Preuss, J. Pang, P. J. Withers and G. J. Baxter: 'Inertia welding nickel-based superalloy: residual stress development', *Metall. Mater. Trans. A*, 2002, **33A**, (10), 3227–3234.
75. D. Deng and H. Murakawa: 'Prediction of welding residual stress in multi-pass butt-welded modified 9Cr–1Mo steel pipe considering phase transformation effects', *Comput. Mater. Sci.*, 2006, **37**, 209–219.